Spontaneous network activity visualized by ultrasensitive Ca^{2+} indicators, yellow Cameleon-Nano

Kazuki Horikawa[1,2,7], Yoshiyuki Yamada[3,4,7], Tomoki Matsuda[1], Kentarou Kobayashi[1], Mitsuhiro Hashimoto[5], Toru Matsu-ura[4], Atsushi Miyawaki[6], Takayuki Michikawa[3,4], Katsuhiko Mikoshiba[3,4] & Takeharu Nagai[1,2]

We report ultrasensitive Ca^{2+} indicators, yellow cameleon-Nano (YC-Nano), developed by engineering the Ca^{2+}-sensing domain of a genetically encoded Ca^{2+} indicator, YC2.60 or YC3.60. Their high Ca^{2+} affinities (K_d = 15–140 nM) and large signal change (1,450%) enabled detection of subtle Ca^{2+} transients associated with intercellular signaling dynamics and neuronal activity, even in 100,000-cell networks. These indicators will be useful for studying information processing in living multicellular networks.

To decipher the principles of information processing in multicellular networks, such as a brain or developing embryo, it is essential to record cellular activity with fine spatiotemporal resolution. Ca^{2+} imaging using synthetic or genetically encoded Ca^{2+} indicators (GECIs)[1,2] is a particularly promising approach because cells display a transient increase in intracellular Ca^{2+} concentration ($[Ca^{2+}]$) when they receive intercellular signals, as in synaptic transmission and hormonal stimulation. Cells have different $[Ca^{2+}]$ at rest and display $[Ca^{2+}]$ transients of different amplitudes upon stimulation that depend on the organism, cell type and stimulus context. Therefore, optimizing the amount of Ca^{2+} indicator and its properties, including its Ca^{2+} affinity and Hill coefficient, is crucial for successful imaging.

Recently, in neuronal imaging, a synthetic Ca^{2+} indicator (Oregon green 488 BAPTA-1 (OGB-1); dissociation constant (K_d) = 170 nM)[1,3] or GECIs (D3cpV, TN-XXL and GCaMP3 with moderate Ca^{2+} affinity; K_d = 600–800 nM)[4–6] have been often used. In these reports, increasing the amount of Ca^{2+} indicator, for example, by bolus loading of OGB-1 to a final concentration of 10–60 μM[3] or by expressing GECIs at 10 μM or more using a viral expression system[4], was necessary to improve the signal-to-noise ratio. However, it is not always possible to load large amounts of indicator: non–animal cells are often impermeant to indicators conjugated to acetoxymethyl esters[7,8], and general transgenic approaches result in low GECI expression[4]. Furthermore, some cells are estimated to have a very low resting $[Ca^{2+}]$ (for example, 30 nM for *Drosophila melanogaster* larval presynaptic motoneuron boutons)[9] and display very small $[Ca^{2+}]$ transients, below the detection limit of low-affinity indicators, in response to action potentials.

An alternative way to detect subtle $[Ca^{2+}]$ changes at low concentrations (<100 nM) is to use a small amount of a high-affinity indicator despite the poor signal-to-noise ratio[10]. In this case, it is crucial to choose an indicator with K_d that is in the middle of the $[Ca^{2+}]$ range to elicit the maximum changes in signal strength. However, only a limited number of high-affinity indicators (K_d < 100 nM; Quin2 and D2cpV)[1,11] are available.

To overcome this problem, we developed high-affinity indicators for sensitive detection of subtle $[Ca^{2+}]$ changes. We derived our new indicators from a fluorescence resonance energy transfer (FRET)-based Ca^{2+} indicator, yellow cameleon 2.60 (YC2.60)[12], which has a large dynamic range and relatively high affinity for Ca^{2+} (K_d = 95 nM, **Supplementary Table 1** and **Supplementary Note 1**). Even though YC2.60 has been used for *in vivo* Ca^{2+} imaging[9], it is not always sensitive enough to detect the endogenous Ca^{2+} dynamics in living cellular networks (see below). The Ca^{2+} affinity of YC2.60 has been previously modified by introducing mutations into the Ca^{2+}-binding pocket of the EF-hand motif in calmodulin (CaM) (E104Q and E31Q in YC3.60 and YC4.60[12], respectively); these modified indicators have a lower Ca^{2+} affinity than YC2.60, which contains wild-type CaM[12,13].

We hypothesized that the flexibility of the linker peptide between CaM and the M13 peptide (**Fig. 1a**) would contribute to the Ca^{2+} affinity because a CaM-M13 fusion peptide connected with a longer linker (5 amino acids with partially deleted M13) has a higher Ca^{2+} affinity (K_d = 18 nM)[14] than that with a shorter linker (Gly-Gly with intact M13; called '+2' with K_d = 80 nM)[15]. We therefore generated yellow cameleon variants with a longer linker, containing three to eight amino acids (designated '+3' to '+8') (**Fig. 1a**). The Ca^{2+} affinity of proteins with longer linker lengths was greater. We named the resulting sensors, high-affinity yellow cameleon proteins or 'YC-Nano'. The protein with the '+3' linker (Gly-Gly-Ser; YC-Nano50) had a K_d of 50 nM, and

[1]Research Institute for Electronic Science, Hokkaido University, Sapporo, Hokkaido, Japan. [2]Precursory Research for Embryonic Science and Technology, Japan Science and Technology Agency, Tokyo, Japan. [3]Japan Science and Technology Agency, International Cooperative Research Project and Solution-Oriented Research for Science and Technology, Calcium Oscillation Project, Saitama, Japan. [4]Laboratory for Developmental Neurobiology, RIKEN Brain Science Institute, Saitama, Japan. [5]Hashimoto Research Unit, RIKEN Brain Science Institute, Saitama, Japan. [6]Laboratory for Cell Function Dynamics, RIKEN Brain Science Institute, Saitama, Japan. [7]These authors contributed equally to this work. Correspondence should be addressed to T.N. (tnagai@es.hokudai.ac.jp).

RECEIVED 23 OCTOBER 2009; ACCEPTED 24 JUNE 2010; PUBLISHED ONLINE 8 AUGUST 2010; DOI:10.1038/NMETH.1488

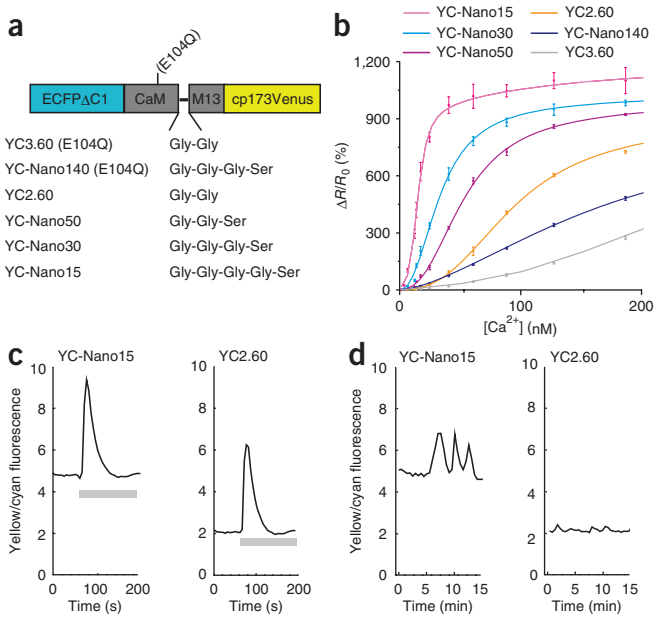

Figure 1 | Design and properties of YC-Nano Ca^{2+} indicators. (**a**) Modified sequences of the peptide linker between CaM and M13. CaM in YC3.60 and Nano140 has the mutation E104Q. M13 is a peptide derived from myosin light chain kinase, which is recognized by Ca^{2+}-bound CaM. ECFPΔC11, enhanced CFP with C-terminal 11 amino acids deleted. cp173Venus, circularly permuted Venus. (**b**) Ca^{2+} titration curves for the indicators. The FRET signal change ($\Delta R/R_0$) is represented as a function of [Ca^{2+}]. Error bars, s.d. (n = 3). (**c**,**d**) Ca^{2+} transients detected with YC-Nano15 and YC2.60 in response to stimulation of *D. discoideum* with 10 μM cAMP (gray bar) (**c**) or with endogenous cAMP during self-organized aggregation (**d**).

the protein with the '+4' linker (Gly-Gly-Gly-Ser; YC-Nano30) had a K_d of 30 nM. Yellow cameleon proteins with a five-to eight-amino-acid linker also had higher affinity than YC2.60. The protein with the '+5' linker (Gly-Gly-Gly-Gly-Ser; YC-Nano15) had the lowest K_d (15 nM); to our knowledge, this indicator had the highest affinity of any GECI reported so far[11] (**Fig. 1b**, **Supplementary Table 1** and **Supplementary Fig. 1**). Linker elongation was also effective for increasing the Ca^{2+} affinity of YC3.60, yielding YC-Nano140 ('+4' linker, Gly-Gly-Gly-Ser; K_d = 140 nM) and YC-Nano65 ('+5' linker, Gly-Gly-Gly-Gly-Ser; K_d = 65 nM) (**Fig. 1b**, **Supplementary Fig. 1** and **Supplementary Table 1**).

Kinetic measurement by stopped-flow fluorometry of YC-Nano140 and YC3.60 revealed that only the rate constant for the 'on' reaction was increased, and the rate of the 'off' reaction remained unchanged (**Supplementary Fig. 2**), suggesting that linker elongation accelerated the Ca^{2+}-induced conformational change of CaM-M13, which might be sterically restricted by the shorter linker (**Supplementary Note 2**). Despite their increased Ca^{2+} affinity, these indicators maintained a large dynamic range (1,250–1,450%) of YC3.60 and YC2.60 (**Supplementary Table 1**), which was achieved by an exceptionally high FRET efficiency (**Supplementary Fig. 3**).

To test the capacity of YC-Nano to detecting subtle [Ca^{2+}] changes in living cells, we used the social amoeba *Dictyostelium discoideum*. These cells exhibit Ca^{2+} transients when stimulated with a chemoattractant molecule, such as cAMP[7]. Because cAMP is also synthesized by the amoeba cells in the aggregation stage, we compared the range of [Ca^{2+}] change in response to both exogenous and endogenous stimuli. We obtained cells stably expressing YC2.60 or YC-Nano15 under the control of the *Dictyostelium Actin15* promoter. The morphology, growth rate and developmental time-course of these cells were unaffected, suggesting that the indicators were not toxic under these experimental conditions (**Supplementary Fig. 4**).

Stimulating YC-expressing *Dictyostlium* with 10 μM cAMP yielded large FRET signal changes, assessed by ratiometric widefield imaging of aggregation-competent cells (**Fig. 1c**). The yellow to cyan fluorescence ratio (R) for the YC-Nano15- and YC2.60-expressing cells changed from 5.0 to 9.5 (ΔR = 4.5) and 2.0 to 6.2 (ΔR = 4.2), respectively. We next determined the amplitude of the Ca^{2+} transients associated with endogenous cAMP signaling, whose spatiotemporal pattern had not been directly visualized by conventional Ca^{2+} indicators. In response to stresses such as nutrient starvation, *Dictyostelium* cells started to aggregate by a cooperative self-organized process, in which propagating waves are established by the repeated synthesis and intercellular relay of cAMP at 6–10-min intervals. Under these conditions, YC-Nano15 showed a clear change in the FRET signal (ΔR = 2.5), whereas that of YC2.60 was almost undetectable (ΔR = 0.2) (**Fig. 1d** and **Supplementary Video 1**), indicating that YC-Nano15, unlike YC2.60, is useful for detecting the small [Ca^{2+}] transients in response to endogenous intercellular signals.

The increased signal strength achieved by optimizing the K_d also allowed us to perform Ca^{2+} imaging on a large spatial scale. The field of view for imaging could be expanded to a millimeter-sized network that included 100,000 *Dictyostelium* cells, in which the aggregation wave was clearly visible as a rotating spiral (**Supplementary Fig. 5** and **Supplementary Video 2**; $\Delta R_{\text{YC-Nano15}}$ = 0.6), indicating that YC-Nano15, unlike YC2.60, was useful for detecting multicellular network

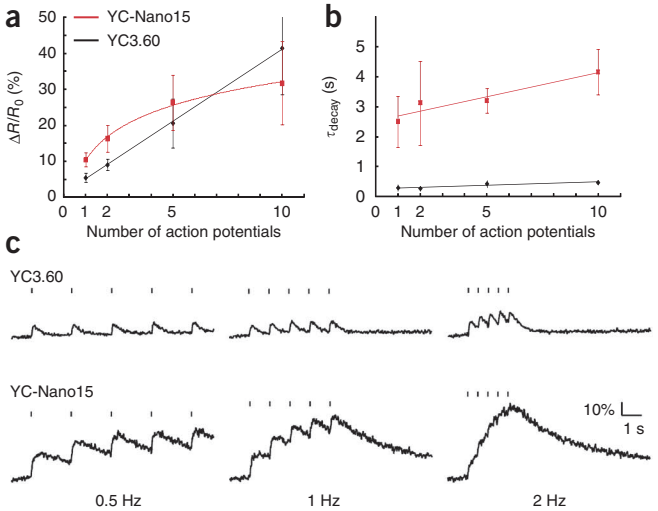

Figure 2 | Comparison of peak amplitude and time constant between YC3.60 and YC-Nano15 expressed in layer 2/3 pyramidal neurons in response to trains of action potentials. (**a**,**b**) Averaged FRET ratio change ($\Delta R/R_0$) (**a**) and time constant for exponential decay (τ_{decay}) (**b**) of the YC3.60 and YC-Nano15 responses versus the number of action potentials in P15–P19 mice. Error bars, s.d. (n = 5 for YC3.60 and n = 7 for YC-Nano15). (**c**) Response of YC3.60 or YC-Nano15 to a train of action potentials delivered at 0.5, 1 and 2 Hz. Bars indicate stimulus timing.

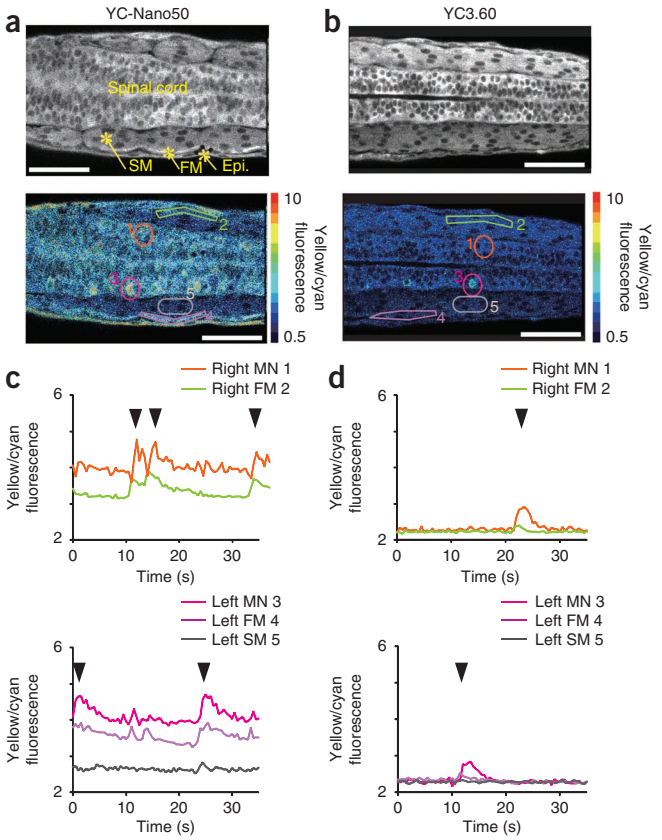

Figure 3 | Spontaneous motor activities in living zebrafish embryos. (**a**,**b**) Confocal images of embryos injected with YC-Nano50 (**a**) or YC3.60 (**b**) proteins (yellow fluorescence signal, horizontal view; right side is at the top and anterior is on the left). Segmented muscles containing slow muscle (SM) and fast muscles (FM) at the inner and outer side of the segment are located between the spinal cord and the epidermis (Epi.). The yellow to cyan fluorescence ratio images are shown at the bottom. Scale bars, 50 μm. (**c**,**d**) Activity of motor neurons (MN), fast muscle (FM) and smooth muscle (SM) during the spontaneous twitching behavior detected with YC-Nano50 (**c**) and YC3.60 (**d**). Alternate firing on the right side (top) and left side (bottom) of the embryos was recorded at 2 Hz for 36 s. Arrowheads indicate the timing of twitching.

activity in self-organized signaling dynamics ($\Delta R_{YC2.60}$ = 0.15, **Supplementary Fig. 6** and **Supplementary Video 3**).

To test YC-Nano performance in a neuronal system (**Supplementary Note 3** and **Supplementary Fig. 7**), we examined its sensitivity to a subtle Ca^{2+} transient triggered by a single action potential. We introduced *YC-Nano15* and *YC3.60* cDNAs into mouse brain on embryonic day 14 using an adenovirus vector and expressed under the control of the *CAG* promoter. We injected current pulses into the soma of whole-cell-patched layer 2/3 pyramidal neurons (acute slices prepared on postnatal day 15–19 (P15–P19)) and detected the FRET signal change at an apical dendrite by two-photon microscopy. To correlate the number of action potentials and FRET signal changes, we elicited a series of current-triggered trains of 1, 2, 5 or 10 action potentials at a frequency of 20 Hz (**Fig. 2a**). For a single action potential the maximal ratio change ($\Delta R/R_0$) for YC-Nano15 was almost double that for YC3.60, but this difference decreased as the number of action potentials increased. We also detected this FRET signal change in the same acute-slice preparation from P72 mice, suggesting that YC-Nano15 could be chronically expressed without serious side effects under these experimental conditions (**Supplementary Table 2** and **Supplementary Fig. 7**). But YC-Nano15 was not suitable for the detection of the large Ca^{2+} transients triggered by high-frequency stimulus, owing to signal saturation and slow decay time (3–4 s) (**Fig. 2b**,**c**).

We also tested YC-Nano performance in the developing zebrafish embryo, which twitches spontaneously (**Supplementary Video 4**). We injected purified YC3.60 and YC-Nano50 proteins into fertilized eggs (**Fig. 3** and **Supplementary Note 4**) and measured the FRET signal change in neuron and muscle populations 20 h later, using conventional confocal microscopy. In embryos loaded with YC3.60, we detected an almost identical baseline FRET signal (R_0 = 2.3) in all cell types (**Fig. 3**). In contrast, YC-Nano50 showed basal ratios, in order from highest to lowest in the epidermis, motor neurons, and fast and slow muscles, suggesting the possibility that these cells have different resting Ca^{2+} levels that cannot be detected with a low-affinity indicator. Furthermore, in addition to the large FRET signal change in the motor neurons and fast muscle detected by both sensors, only YC-Nano50 detected the subtle FRET signal change in slow muscle. This result demonstrated that the newly developed indicators are useful for detecting the spatiotemporal patterns of *in vivo* cellular activities, including subtle Ca^{2+} transients at low concentrations (**Supplementary Videos 5** and **6** and **Supplementary Note 5**).

The YC-Nano ultrasensitive Ca^{2+} indicators can detect the subtle Ca^{2+} transients associated with spontaneous network activity and reveal cell-type-dependent and stimulation-dependent differences in both the resting Ca^{2+} level and the amplitude of Ca^{2+} transients. This indicates that the selection of indicators with an appropriate K_d is essential for *in vivo* Ca^{2+} imaging, and indicators with finely tuned K_d values optimized to detect [Ca^{2+}] from 10 nM to 100 nM would enable precise and reliable Ca^{2+} imaging, even in large-scale cellular networks.

METHODS

Methods and any associated references are available in the online version of the paper at http://www.nature.com/naturemethods/.

Accession codes. GenBank, EMBL Nucleotide Sequence Database and DNA Databank of Japan: GU071083, GU071084, GU071085, HM145948 and HM145949 (nucleotide sequences encoding YC-Nano15, YC-Nano30, YC-Nano50, YC-Nano65 and YC-Nano140, respectively).

Note: Supplementary information is available on the Nature Methods website.

ACKNOWLEDGMENTS

We thank A. Nagasaki and Y. Kuramoto for instruction and assistance with the experiment using *Dictyostelium* cell, T. Kotani and S. Higashijima for assistance and instruction on fish embryo imaging, and T. Shimogori for instruction on *in utero* injection. This work was partly supported by a Grant-in-Aid for Young Scientists (A) of the Japan Society for the Promotion of Science and Scientific Research on Advanced Medical Technology of the Ministry of Labor, Health and Welfare of Japan to T.N. and a grant from Precursory Research for Embryonic Science and Technology of the Japan Science and Technology Agency to T.N. and K.H.

AUTHOR CONTRIBUTIONS

K.H. and T.N. invented YC-Nano variants. Y.Y., M.H., A.M., T. Michikawa and K.M. established the method of the expression of Ca^{2+} indicators in neurons using adenoviral vectors; K.H. and T. Matsuda performed experiments other

than electrophysiology and Ca^{2+} imaging in brain slices. K.H. and T. Matsu-ura performed stopped-flow spectrometry. Y.Y. performed electrophysiology and Ca^{2+} imaging in brain slices; K.H., K.K., Y.Y., T. Michikawa and T.N. analyzed data. K.H., Y.Y., T. Michikawa and T.N. wrote the manuscript. T.N. supervised the study.

COMPETING FINANCIAL INTERESTS

The authors declare no competing financial interests.

Published online at http://www.nature.com/naturemethods/.
Reprints and permissions information is available online at http://npg.nature.com/reprintsandpermissions/.

1. Paredes, R.M., Etzler, J.C., Watts, L.T., Zheng, W. & Lechleiter, J.D. *Methods* **46**, 143–151 (2008).
2. Kotlikoff, M.I. *J. Physiol. (Lond.)* **578**, 55–67 (2007).
3. Stosiek, C., Garaschuk, O., Holthoff, K. & Konnerth, A. *Proc. Natl. Acad. Sci. USA* **100**, 7319–7324 (2003).
4. Wallace, D.J. *et al. Nat. Methods* **5**, 797–804 (2008).
5. Mank, M. *et al. Nat. Methods* **5**, 805–811 (2008).
6. Tian, L. *et al. Nat. Methods* **6**, 875–881 (2009).
7. Abe, T., Maeda, Y. & Iijima, T. *Differentiation* **39**, 90–96 (1988).
8. Zhang, W.H., Rengel, Z. & Kuo, J. *Plant J.* **15**, 147–151 (1998).
9. Hendel, T. *et al. J. Neurosci.* **28**, 7399–7411 (2008).
10. Yasuda, R. *et al. Sci. STKE* **2004**, pl5 (2004).
11. Palmer, A.E. & Tsien, R.Y. *Nat. Protoc.* **1**, 1057–1065 (2006).
12. Nagai, T., Yamada, S., Tominaga, T., Ichikawa, M. & Miyawaki, A. *Proc. Natl. Acad. Sci. USA* **101**, 10554–10559 (2004).
13. Miyawaki, A. *et al. Nature* **388**, 882–887 (1997).
14. Martin, S.R. *et al. Biochemistry* **35**, 3508–3517 (1996).
15. Porumb, T., Yau, P., Harvey, T.S. & Ikura, M. *Protein Eng.* **7**, 109–115 (1994).

ONLINE METHODS

Gene construction. The peptide linker sequence between the CaM and M13 domains in YC2.60 and YC3.60 was replaced with $(Gly)_n$-Ser flexible linkers; the changes were made in the sequences encoding these fusions by PCR. For sequences of proteins with linkers composed of 3–5 amino acids, the cDNA encoding CaM was amplified with a GCATGC-tagged forward primer and $(GGN)_{n-1}$GGATCC-tagged reverse primer. The cDNA of M13-cp173Venus was amplified with a GGATCC-tagged M13 forward primer and GAATTC-tagged cp173Venus reverse primer. After ligating the cDNA fragments encoding CaM and M13-cp173Venus at the BamHI site, the full-length cDNA of yellow cameleon (YC) was cloned into $pRSET_B$ (Invitrogen) by connecting a cDNA encoding ECFPΔC11 (enhanced cyan fluorescent protein with the C-terminal 11 amino acids deleted). To purify the recombinant proteins, strep tag II (IBA) was attached to the C terminus of YC, through an arginine–aspartic acid linker.

Protein expression and purification. *Escherichia coli* (JM109(DE3)) transformed with $pRSET_B$ containing the cDNA for YC variants was grown for 60 h at 23 °C with gentle shaking at 150 r.p.m. The recombinant proteins were sequentially purified by a Ni-NTA column (Qiagen) and StrepTactin beads (Qiagen), followed by gel filtration using a PD-10 column (GE Healthcare) to exchange the buffer with 5 mM HEPES, pH 7.2.

***In vitro* Ca^{2+} titration.** The emission spectra of the recombinant YC variants at 0.3 μM were measured by excitation at 430 nm using an F-2500 fluorescence spectrophotometer (Hitachi). Ca^{2+} titrations were performed by the reciprocal dilution of Ca^{2+}-saturated and Ca^{2+}-free buffers containing MOPS (10 mM), KCl (100 mM) and EGTA (10 mM) or EDTA-OH (10 mM) with or without 10 mM Ca^{2+} added as $CaCO_3$ at pH 7.2, room temperature (23–25 °C)[16]. The final concentration of free Ca^{2+} in reciprocally diluted solutions (24 solutions between 1.4 nM and 3 mM) was precisely determined individually using a Ca^{2+}-sensitive electrode (Metrohm)[17], which was calibrated with standard Ca^{2+} solutions purchased from Orion Research. The averaged data from three independent measurements was fitted to the Hill equation in a two-site model using Origin7 (OriginLab). To determine the FRET efficiency, 0.3 μM YC-Nano15 digested with proteinase K (final concentration 1 μg ml^{-1}) for 2 h at 37 °C in the presence or absence of Ca^{2+} was also subjected to the spectrum measurement.

Kinetic measurement. Measurements of the Ca^{2+}-binding kinetics of YC were performed as described previously[13,18]. Briefly, a stopped-flow photometry system consisting of an RX.2000 rapid mixing stopped-flow unit (Leatherhead) and FP-750 spectrophotometer (JASCO) were used. The time course of the yellow fluorescence emission change (excited with 430 nm) from Ca^{2+}-free to a predetermined Ca^{2+} concentration was measured at 1,000 Hz. The time constants for the 'on' reaction were calculated by performing curve fitting for a single exponential equation. The association and dissociation rate constants (k_{on} and k_{off}) were determined by fitting the data to the equation $k_{obs} = k_{on}[Ca^{2+}] + k_{off}$.

Culture and imaging of *D. discoideum*. YC variants were expressed in Ax2 cells under the control of the Actin15 promoter. Briefly, the cells were electroporated with pBig expression vectors[19] and transformants were selected in HL5 medium containing 10 μg ml^{-1} G418 (Invitrogen). To initiate the self-organized aggregation, 10^8 cells were starved in development buffer (5 mM MES, 5 mM $CaCl_2$ and 5 mM $MgCl_2$, pH 6.5) at 10^7 cells ml^{-1}. For smaller-scale observation, aggregation-competent cells suspended in development buffer were plated on a glass-bottom dish (10^5 cell cm^{-2}) and imaged with a widefield epifluorescence inverted microscope (TE2000, Nikon) equipped with 10× objectives (PlanApo, numerical aperture (NA) 0.45; Nikon). The samples were illuminated with a 100-W mercury arc-lamp through 6.25% and 12.5% neutral density filters and a 438/20 excitation filter (Semrock). The fluorescence signals were split into two channels using the W-view system (Hamamatsu) to detect the donor cyan fluorescence and acceptor yellow fluorescence signals simultaneously through 480AF30 and 535DF25 interference filters (Omega), respectively, using an electron-multiplying charge-coupled device (EM-CCD) camera (ImagEM, Hamamatsu), every 3 s. For the large-scale observations, starved cells (2.5×10^6 cell cm^{-2}) were plated on a glass-bottom dish covered with a thin agarose layer and were imaged with 4× objectives (PlanApo, NA 0.2; Nikon). The cyan and yellow fluorescence signals were sequentially captured every 15 s by using an emission filter changer (Ludl Electronic Products). The doubling time was determined for the suspension culture in 20 ml of HL5 containing G418 (10 μg ml^{-1}) shaken at 135 r.p.m.

Expression of YCs in neocortical layer 2/3 pyramidal neurons. YC3.60 and YC-Nano15 were subcloned into a cosmid vector carrying the CAG promoter (cytomegalovirus enhancer and β-actin promoter), woodchuck hepatitis virus post-transcriptional regulatory element and bovine growth hormone polyadenylation signal. The BspT104I-digested cosmid DNA was transfected into human embryonic kidney 293 cells (kindly provided by the Cell Resource Center for Biomedical Research, Institute of Development, Aging and Cancer, Tohoku University), and recombinant adenovirus was generated by the full-length DNA transfer method[20,21]. Purified recombinant adenovirus was injected into the lateral ventricle of ICR mice on embryonic day 14 (**Supplementary Note 3**).

Electrophysiology and Ca^{2+} imaging in acute brain slice. All experimental procedures were performed in accordance with the guidelines of the Animal Experiment Committee of the RIKEN Brain Science Institute. Mice were decapitated after ether anesthesia, and oblique parasagittal slices (300 μm) were prepared on postnatal day 15 or later, as described previously[22]. Whole-cell patch-clamp recording from the layer 2/3 pyramidal neurons was performed at 31–35 °C. The patch pipettes were filled with the internal solution containing 140 mM K-gluconate, 4 mM NaCl, 10 mM HEPES, 4 mM Mg-ATP, 0.3 mM Na-GTP and 5 mM Na_2-phosphocreatine (pH 7.3 titrated with KOH, 285–295 mOsm). Slices were perfused at ~2 ml min^{-1} with artificial cerebral spinal fluid (ACSF) containing 125 mM NaCl, 2.5 mM KCl, 25 mM $NaHCO_3$, 25 mM D-glucose, 1.25 mM NaH_2PO_4, 2 mM $CaCl_2$ and 1 mM $MgCl_2$. ACSF was constantly bubbled with carbogen. Action potentials were elicited by brief somatic current pulses (1–3 nA, 2 ms). Electrophysiological signals were acquired with a MultiClamp 700B (Molecular Devices) and AxoGraphX software (AxoGraph Scientific).

CFP and yellow fluorescent protein emission was acquired in line-scan mode (approximately 200 Hz) with a two-photon

laser-scanning microscope (FV300; Olympus) equipped with a 60× water-immersion objective (LUMPlan Fl/IR NA 0.90; Olympus). A Ti:sapphire laser (Maitai VF-TIM, Spectra-Physics) tuned to 840 nm was used for excitation. Cyan and yellow fluorescence signals were acquired with a dichroic mirror (510 nm, Chroma) and band-pass filters (480/40 nm and 535/30 nm for cyan and yellow fluorescence, respectively; Chroma). The photomultiplier dark current was subtracted from all traces. The fractional change of the yellow to cyan fluorescence emission ratio ($\Delta R/R_0$) was calculated. The mean baseline fluorescence ratio (R_0) was defined as the mean ratio of the approximately 1-s window immediately before stimulus onset. The signal-to-noise ratio was calculated as the peak amplitude divided by the baseline noise, where the peak amplitude was the maximum value of the $\Delta R/R_0$ trace filtered with a 35-ms moving window, and the baseline noise was the s.d. of the raw trace during the baseline period, when R_0 was calculated. Statistical difference was assessed using a two-tailed Student's *t*-test ($P = 0.05$). Data analysis was performed with AxoGraphX, Igor Pro 6 (WaveMetrics), NeuroMatic (http://www.neuromatic.thinkrandom.com/), Fluoview (Olympus), ImageJ (US National Institutes of Health) and Excel (Microsoft) software.

Fish culture and imaging. *Danio rerio* obtained from a pet shop were kept under a 14/10-h light-dark cycle, as described elsewhere[23]. The eggs were injected with purified protein (100 μM) to yield final cellular concentrations of around 5 μM and allowed to develop at 28.5 °C. The concentration of loaded indicator was estimated from the emission intensity of yellow fluorescent protein after excitation with a 515-nm laser line under confocal microscopy. For imaging, the embryos were mounted in a glass-bottom dish filled with 2% low-melting-point agarose. Ratiometric imaging was performed with a confocal microscope (A1, Nikon) equipped with water immersion 60× objectives (ApoVC, NA 1.20, Nikon). The samples were excited with a 458-nm multi-argon ion laser line, and images captured through emission filters (482/35 for CFP and 540/30 for yellow fluorescence) were collected at 2 Hz.

16. Tsien, R.Y. & Pozzan, T. *Methods Enzymol.* **172**, 230–262 (1989).
17. Bers, D.M. *Am. J. Physiol.* **242**, C404–C408 (1982).
18. Matsu-ura, T. *et al. J. Cell Biol.* **173**, 755–765 (2006).
19. Nagasaki, A., de Hostos, E.L. & Uyeda, T.Q.P. *J. Cell Sci.* **115**, 2241–2251 (2001).
20. Mizuguchi, H. & Kay, M.A. *Hum. Gene Ther.* **9**, 2577–2583 (1998).
21. Fukuda, H., Terashima, M., Koshikawa, M., Kanegae, Y. & Saito, I. *Microbiol. Immunol.* **50**, 643–654 (2006).
22. Davie, J.T. *et al. Nat. Protoc.* **1**, 1235–1247 (2006).
23. Westerfield, M. The zebrafish book. A guide for the laboratory use of zebrafish (*Danio rerio*). 4th edn. (Univ. of Oregon Press, Eugene, 2000).

doi:10.1038/nmeth.1488